ESA'S COLLISION AVOIDANCE SERVICE: CURRENT STATUS AND SPECIAL CASES

Klaus Merz[(1)], Jan Siminski[(1)], Benjamin Bastida Virgili[(1)], Vitali Braun[(1)], Sven Flegel[(1)], Tim Flohrer[(1)], Quirin Funke[(1)], Andre Horstmann[(1)], Stijn Lemmens[(1)], Francesca Letizia[(1)], Frazer Mclean[(1)], Silvia Sanvido[(1)], Volker Schaus[(1)]

[(1)] Space Debris Office, ESA/ESOC, Robert-Bosch-Str. 5, 64293 Darmstadt, Germany, firstname.lastname@esa.int

ABSTRACT

ESA's Space Debris Office (SDO) provides operational collision avoidance support to internal ESA missions as well as external partners. The support covers missions in low-Earth orbit and highly eccentric ones, but also special cases such as a conjunction analyses for Earth flybys of interplanetary missions.

This diversity of missions often requires the development of custom solutions to account for operational reality. An example custom analysis was needed when large acquisition manoeuvres are performed and lead to increased state uncertainties and ultimately a collision probability dilution. A new metric is presented, which overcomes the limitation of the traditional collision probability by allowing a position shift. The method and its limitation in the operational context are discussed.

The overall processing chain is currently upgraded and modernized in order to cope with expected future data loads and to be able to ingest conjunction warnings from multiple surveillance data providers. The chain includes conjunction event detection, collision risk assessment and visualization, orbit and covariance propagation, process control and data handling.

This paper will outline the new developments, present results from custom analyses such as the new metric, as well as provide the most recent statistics on conjunction events.

1 INTRODUCTION

Severe fragmentation events, such as the destruction of Fengyun-1C in 2007, the Iridium-33/Cosmos-2251 collision in 2009, and the Briz-M explosions of 2012, resulted in a significant number of additional objects to the debris population. The events demonstrated the need to consider collision avoidance as part of routine operations to all mission operators and should be considered as good practice in view of space debris mitigation. Operational conjunction analyses and collision avoidance activities at ESA started already before these major events for the ERS-2 and Envisat spacecraft and nowadays concentrate on ESA's Earth Explorer missions, the Copernicus' Sentinel spacecraft in LEO, ESA's science missions in HEO as well as on external partner spacecraft – see Figure 1 for a history of spacecraft fully supported by the operational process. Additionally, several other missions were covered in the past under varying support level and duration (e.g. LEOP): Proba-1, -V, Galileo/Giove, METOP-A/-B/-C, MSG-3/4, Artemis, Lisa-Pathfinder, Sentinel-6A.

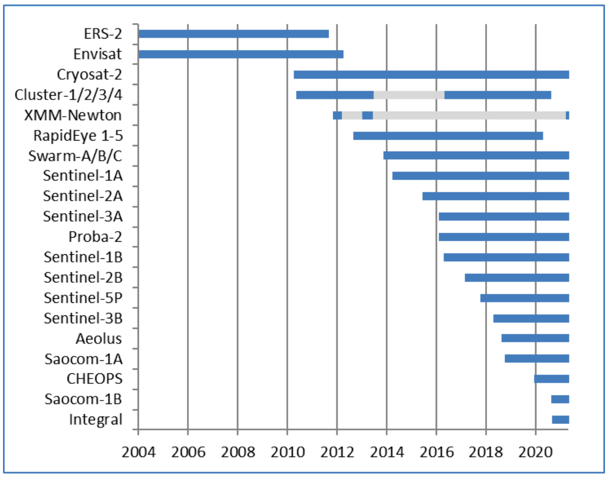

Figure 1: Spacecraft under full coverage of operational conjunction assessment service

Initially, close conjunctions were identified by an internal screening of mission orbits versus the public TLE catalogue provided by USSTRATCOM. In the aftermath of the Iridium-33/Cosmos-2251 collision event, USSTRATCOM has started to provide dedicated data messages based on high precision SP catalogue. ESA's collision avoidance process has evolved significantly since then, exploiting all the features that these messages offer to provide an extended service to missions. Today, conjunction data messages (CDMs) provided by the US 18th Space Control Squadron are retrieved and analysed in an automated way, returning the approach details and an estimate of the associated collision probability.

Conjunction events showing high risks are further assessed and mission-specific processes are in place for decision-taking and manoeuvre recommendation. A key part of these are thresholds in collision probability to decide on the need to perform an avoidance manoeuvre, but of course operational constraints also have to be taken into account, mainly the time needed to prepare and

Proc. 8th European Conference on Space Debris (virtual), Darmstadt, Germany, 20–23 April 2021, published by the ESA Space Debris Office
Ed. T. Flohrer, S. Lemmens & F. Schmitz, (http://conference.sdo.esoc.esa.int, May 2021)

execute a potential avoidance manoeuvre driving the time a decision has to be taken on the avoidance manoeuvre parameters and whether to execute it or not (often this final GO/NOGO manoeuvre decision can be taken later).

The question remains what a good reaction threshold actually is. In order to analyse this, it is convenient to use ESA's ARES [1,2,3] tool (within the DRAMA tool suite). It allows the estimation of overall collision risk as well as the annual frequency of close approaches with risks above levels selected by the user as a function of spacecraft size as well as the quality and age (time to event) of the secondary (catalogue) orbit information. It is thus possible to trade-off ignored risk against avoided risk via selecting the risk threshold at the cost of a number of manoeuvres obtained as frequency of events having higher risk than the selected threshold. A more detailed discussion of this approach, its drivers and typical ESOC approach can be found in [4].

In this paper we present the current operational process and its ongoing and planned upgrades in section 2. In section 3 we present two special support cases and section 4 summarises some relevant statistics of the collision avoidance process covering the past few years.

2 CURRENT OPERATIONAL PROCESS

In this section we give a brief description of ESA's current collision avoidance process, followed by a description of its upgrades which are currently under development.

Today, the collision avoidance process is based on operational orbit and manoeuvre information for the ESA and partner spacecraft (targets) and conjunction data messages (CDMs) provided by the US 18th Space Control Squadron (18SPCS) which performs the space surveillance mission for the U.S. Space Force, and provides foundational SSA for the U.S. government and global space partners through the SSA Sharing Program.

The CDMs cover details on conjunctions between objects contained in the US catalogue (chasers) and the target trajectories, in particular time of closest approach (TCA), separations, state vectors and covariances at TCA as well as auxiliary information on the orbit determination setup and quality. Due to a data sharing agreement between the US Strategic Command (USSTRATCOM) and ESA, signed on October 30th, 2014, the SDO has access to CDMs covering larger volumes around the target trajectories and longer lead times.

In view of the large number of CDMs and the associated risk analyses, a database-centric approach has been developed: All CDMs and risk analysis results are stored in a database. The database is also used as the backbone for a web-based tool, which consists of a visualisation component and a collaboration tool that facilitates the status monitoring and task allocation within the support team as well as the communication with the control team (SCARF). The visualisation component further supports the information sharing by displaying target and chaser motion over time along with the involved uncertainties. This web-based solution optimally meets the needs for a concise and easy-to-use way to obtain a situation picture in very short time, and the support for third party missions not operated from ESOC.

The processing chain is summarised in Figure 2 and discussed in the following. Herein the grey shaded part of the processing chain is fully automated.

CDMs are downloaded automatically and the associated risks computed using the CORAM [5] software and object geometry taken from DISCOS. Two probabilities are computed in this process: one based on target and chaser state and covariance given within the CDM, and a 2nd one using only the chaser data from the CDM and flight dynamics data for the target spacecraft. The resulting data set is stored in the central database (top process flow in the grey area of Figure 2).

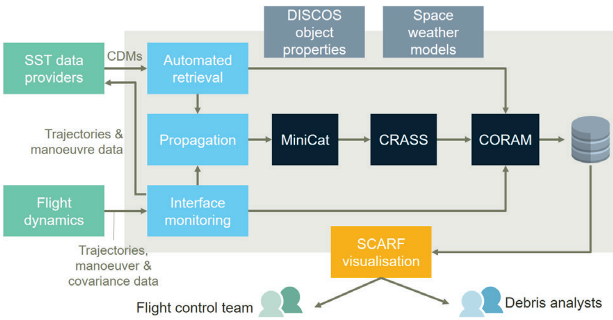

Figure 2: Current processing chain of ESA's operational conjunction assessment system

Collision probabilities are also computed whenever flight dynamics data are updated, i.e. using the chaser data from the latest CDM and target data from the new operational data. Again, the resulting data set is stored in the central database (flow at the bottom of the grey area of Figure 2).

Propagating the chaser state vectors contained in the CDMs with DISCOS information on the physical object properties a temporary local "mini-catalogue" of objects close to our target spacecraft is obtained. The generation of this mini-catalogue is triggered automatically after every CDM retrieval. It is used for finding close approaches using CRASS [6] and computing their collision probabilities using CORAM based on the operational target trajectories. This process is triggered by the availability either of the updated mini-catalogue (due to new CDMs) and whenever new ephemeris becomes available from the flight dynamics team, be it due to updated orbit determination or due to incorporation of planned manoeuvres (flow in the middle of the grey area of Figure 2). While this process typically does not find additional conjunctions as long as the operational ephemeris is close to the one of the catalogue of the surveillance system, it can be useful in case of manoeuvres which have not been screened (yet) by the 18SPCS.

This processing chain in particular allows screening of manoeuvre trajectories for close approaches without waiting for the results of an extra screening request to 18SPCS as long as manoeuvres are small enough such that the difference to the no-manoeuvre trajectory is smaller than the screening volume (18SPCS is kept informed of manoeuvres in any case).

As mentioned, this part of the processing chain is fully automated, but the analyst can also manually trigger extra analyses, e.g. running (avoidance) manoeuvre ephemeris against the mini-catalogue and inserting the resulting data sets into the database and display them on web frontend.

As mentioned above conjunction events showing high risks are further assessed and mission-specific processes are in place for decision-taking and manoeuvre recommendation. This is supported by a manoeuvre optimisation component of the CORAM software which also runs as part of the automatic sequence for conjunctions showing high risk in a default configuration suitable for typical manoeuvre scenarios, but can be configured and run by the analyst according to specific needs.

More details on the algorithms, database, and analyst frontends are given in [7]. The system has seen feature updates and maintenance since then, but no major change in underlying technology has been implemented. The past evolution of the process is covered more extensively by earlier work (e.g. [8]).

2.1 Upgrade of the system

The current processing chain connects the database and various numerical software packages such as CRASS and CORAM as well as auxiliary tools via a collection of interconnected scripts of different types (shell, Perl, Python) triggered by crontabs. This system has become increasingly complex over time e.g. due to many special cases to be covered such as dedicated interfaces for various missions and tweaks to prioritise tasks and increase performance. This complexity has led to significant effort to maintain the system but also significant training needs for the analyst staff operating the system.

It has therefore been decided to refactor this processing chain and related tasks, build a convenient web-based User Interface (UI) for controlling the process, embed procedures in this UI, improve fault tolerance and repeatability and increase performance and scalability.

To achieve this, the new framework is built on distributed computing using Celery [9] task queues with a custom workflow and job implementation. Workflows control the order of jobs, which perform the actual work, and track their progress; they also support interaction with the jobs, like changing priorities. A central scheduler is responsible for starting workflows and keeping track of their status. The system is designed to be scalable as new worker nodes can be easily added and jobs can be worked on in parallel.

A web-based UI using Flask [10] in the backend and React [11] in the frontend is being developed, which allows the debris analyst to monitor and control the process chain – see Figure 3 for an early version giving access to a few representative workflows.

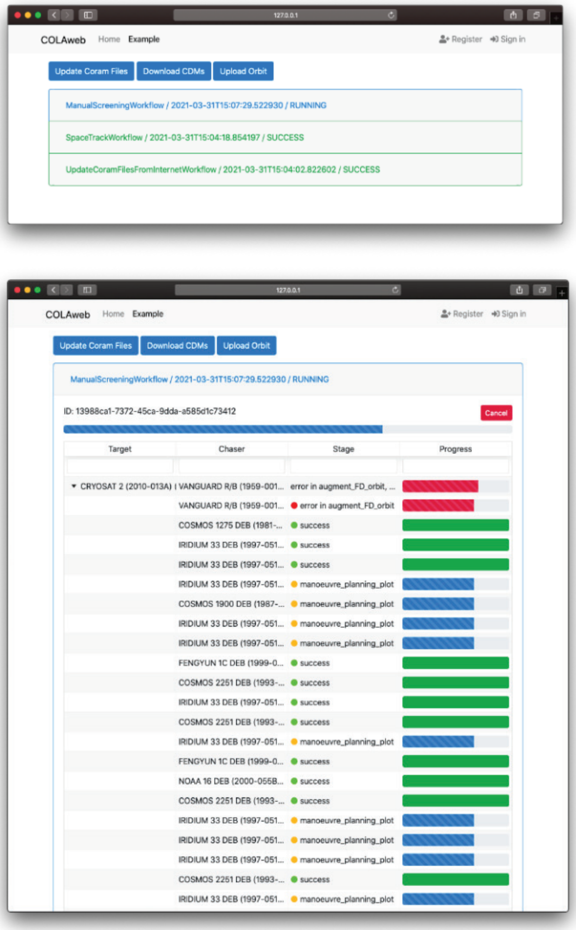

Figure 3: Early version of UI to monitor and control workflows of refactored processing framework

A significant part of the development of the new framework and its workflows and jobs consists in encapsulating clear interfaces to the functionalities provided by the core numerical tools. Therefore, this activity also paves the way for the opportunity to replace legacy code one by one, once the development of the new framework is completed. It is foreseen to rebase legacy applications via components and enhancements of the astrodynamics platform currently being developed by

ESOC FD with contributions from SDO.

Other upgrades planned for the conjunction assessment system focus on enhancements of the SCARF frontend, in particular covering improved plotting features, a comprehensive multi-mission view and features dealing with integration of different CDM providers (e.g. from EUSST and commercial providers). It is also planned to integrate results from ongoing and precursor activities of the CREAM cornerstone of ESA's Space Safety Programme, in particular to display event classifiers and predictors to the analyst, such as criticality indicators or covariance predictors as they are being developed by assessing the CDMs collected in the past years via statistical and machine learning techniques (e.g. with the challenge described in [12]).

3 SPECIAL CASES

The routine collision avoidance operations are mostly automated in the above-described processing chain. However, the SDO also performs custom analyses to support non-standard scenarios, such as an Earth flyby of interplanetary missions or special manoeuvre campaigns. The following sections summarise methodology and findings for two of such cases.

3.1 BepiColombo Earth flyby

BepiColombo is a joint mission between ESA and JAXA to explore the planet Mercury. Its cruise trajectory includes one flyby of the Earth, two of Venus and six of Mercury itself, before orbit insertion in December 2025 [13]. The first flyby of Earth was needed to deflect the spacecraft into the inner solar system. The time of the closest approach between Earth and the spacecraft was April 10th, 2020 at 04:25 UTC.

During its flyby the spacecraft reached a minimum altitude of 12684 km. Around 2 hours before and after the close approach, the spacecraft passed through the protected Geosynchronous Region (42164 ± 200 km distance to Earth's centre and latitude between ± 15 degrees [14]).

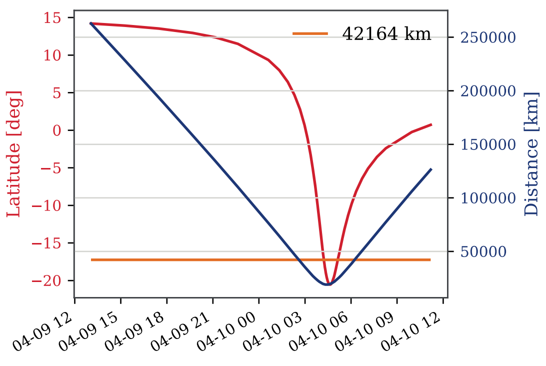

Figure 4: BepiColombo flyby distance to Earth's centre and latitude

As the spacecraft was able to modify its flyby trajectory to avoid a collision, a conjunction assessment was agreed with the mission. For this purpose, an ODR was put in place with 18SPCS to provide CDMs for a given trajectory. The screening has been performed on April 7th, 2020 and returned no close approaches within the deep-space screening volume (40 x 77 x107 km radial, in-track, cross-track direction). Additionally, the SP catalogue and analyst TLEs from space-track.org have been used in an internal screening to identify the closest objects. The results are shown in Table 1. Again, no critical approaches have been identified and consequently there was no need to modify the flyby trajectory.

Table 1: Closest approaches of BepiColombo during Flyby

Object	TCA	Min. dist.
Beidou DW 54	2020-04-10T02:45:33	760 km
Blok-2BL	2020-04-10T05:15:01	790 km
Ariane 5 oper. debris	2020-04-10T03:44:20	920 km

The operational tools for this assessment had to be modified to allow the screening of a hyperbolic trajectory. In particular, typical apogee and perigee filtering [15] and the minimum distance search step size selection often assume an elliptic orbit. Both could be solved by accounting for the minimum Earth approach distance and velocity.

3.2 Large acquisition manoeuvres

During nominal operations, the collision probability is used to assess if any avoidance actions are needed or not. In the presence of high orbital uncertainties, it becomes difficult to interpret this quantity as a safety criterion as higher uncertainties potentially reduce the likelihood of a collision. This property, the so-called dilution, has been studied in detail [16, 17]. In the typical scenario, the orbital uncertainties of poorly tracked debris will drive the dilution as the target orbit is well determined using GNSS derived data or ranging. Conservative approaches have been proposed to overcome this limitation e.g. by assessing the situation based on the maximum possible collision probability (e.g. using covariance scaling) or by testing if the miss-distance is outside a certain confidence region [17]. However, it can also be argued that this population of poorly tracked objects and the corresponding risk can be accepted the same way the risk of any untracked piece of debris currently is [16].

During the initial acquisition, a spacecraft will often perform large manoeuvres to reach the target orbit. In case of Sentinel-3B, these manoeuvres could become as large as ~2 m/s. The history of all manoeuvres larger than 1 m/s is summarised in Table 2.

Table 2: Sentinel-3B large acquisition manoeuvres

Manoeuvre epoch	Magnitude
2018-05-08T09:24:27	1.0 m/s
2018-05-08T11:05:38	1.0 m/s
2018-05-10T11:31:00	1.6 m/s
2018-05-24T13:01:25	2.1 m/s
2018-05-29T05:04:10	2.0 m/s
2018-05-30T13:05:35	1.4 m/s

The execution of manoeuvres introduces uncertainties in the orbital prediction, especially during the initial phase of a spacecraft mission. The so-called mechanisation error is modelled to account for the predicted deviation between the actual $\Delta\boldsymbol{v}$ and planned manoeuvre $\Delta\widetilde{\boldsymbol{v}}$

$$\Delta\boldsymbol{v} = \Delta\widetilde{\boldsymbol{v}} + \boldsymbol{\epsilon}_{\Delta v} \ .$$

The error $\boldsymbol{\epsilon}_{\Delta v}$ modelling in the ESA operational process accounts for uncertainties in the manoeuvre modulus (e.g. when the burn period cannot be exactly timed) and a pointing error (e.g. when the attitude of the spacecraft is not perfectly known). The overall error is assumed to be distributed according to a multivariate normal distribution, i.e. $\boldsymbol{\epsilon}_{\Delta v} \sim \boldsymbol{N}(0, \boldsymbol{C}_{\Delta v})$, where the covariance matrix $\boldsymbol{C}_{\Delta v}$ is added to the velocity components of the state covariance at the time of the manoeuvre during the propagation.

In-track manoeuvres are the most efficient way to raise the orbit. For simplicity, the analysis focuses on this component rather than the full covariance. The uncertainty in the in-track component σ_T of the orbital state vector w.r.t. the manoeuvre modulus error σ_M can be approximated with

$$\sigma_T \approx 3\ \Delta t\ \sigma_M \ ,$$

where Δt is the time since the manoeuvre execution epoch and assuming small uncertainty at the start of the propagation interval. This accumulates to ~2.8 km in-track uncertainty growth per day for a 2 m/s manoeuvre assuming a 1.5% error σ_M during propagation. An example covariance evolution using the operational numerical state and covariance prediction assuming the same modulus error is shown in Figure 5. For the sake of better visualisation, the figure shows only the uncertainty envelope over time, i.e. the maximum value per revolution. In reality, the position uncertainty will periodically decrease whenever the manoeuvre execution location along the orbit is approached.

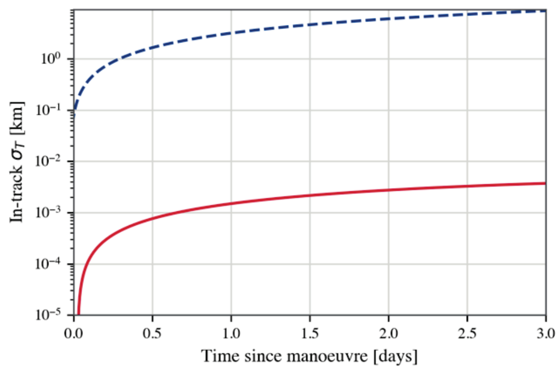

Figure 5: In-track uncertainty evolution after the execution of a 2 m/s in-track manoeuvre (blue dashed line) and without (red solid line) for Sentinel-3B using numerical integration.

In case of such large manoeuvres, the dilution region can be reached due to the target uncertainty and not because of poorly tracked debris. However, after the calibration of the manoeuvre, e.g. when receiving new GNSS data, the uncertainty reduces again to the nominal case (e.g. ~10 m level). This raises the question what decision metric should be used in this scenario as an overly conservative metric might lead to manoeuvre cancelations and effectively prevents any target orbit acquisition.

3.2.1 Confidence region approach

An often-proposed solution to the dilution is to assess if the miss-distance is outside a certain confidence region [16,17]. The advantage of the approach is that it can be easily interpreted, i.e. the sphere defined by the combined hard body radius (HBR) of the two objects is forced to be outside a certain percentile of the miss distance distribution. In case of a miss distance vector $\boldsymbol{\Delta r}$, a confidence region can be constructed with a 3-D ellipsoid covering a certain fraction of the multivariate normal distribution, e.g. 99.9%. The combined covariance $\boldsymbol{C}_{\Delta r}$ is the sum of the target and chaser position covariances. The approach is visualised in Figure 3.

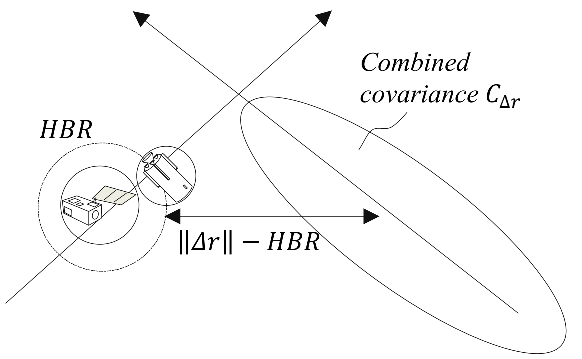

Figure 6: Visualisation of confidence region approach

A statistical distance metric

$$d^2 = \boldsymbol{u}^T \boldsymbol{C}_{\Delta r}^{-1} \boldsymbol{u}$$

is used to test if two trajectories are within the selected confidence interval, where the corrected miss distance vector is

$$\boldsymbol{u} = \Delta \boldsymbol{r} - HBR \frac{\Delta r}{\|\Delta r\|} .$$

The minimum of d^2 (which is not necessarily the same as the minimum miss-distance at TCA) is then tested using the χ^2-distribution with 3 degrees of freedom. The cumulative probability density function value $F_3(d^2)$ defines the percentile of the error ellipsoid which just touches the HBR sphere. The threshold on d^2 would be 16.27 in case of a 99.9 % percentile.

Reference [16] discusses how this metric is leading to a large number of additional events which would require avoidance actions. This motivates the definition of a less restrictive approach and then to compare it against the confidence region.

3.2.2 Worst-case scenario approach

When screening a trajectory with a planned manoeuvre, the conjunction events after the manoeuvre epoch will be affected by the large uncertainty. If the collision probability is diluted, these events would be regarded as harmless. As soon as new data after the manoeuvre is used for a trajectory update, the uncertainty will decrease to nominal values which then can lead to a sudden increase of risk levels and even the appearance of high-risk events, i.e. the collision probability rises above the reaction threshold. These events can then be too close to allow a quick reaction.

The post-manoeuvre orbit determination covariance is approximately known from historic orbit comparison [18]. Instead of using a fixed value for this covariance, a confidence interval allows scaling the covariance to find the maximum reasonable collision probability. Covariance scaling is typically used to account for the uncertainty of the uncertainty. Reference [19] suggests to visualise the collision probability topography as a function of the miss-distance and covariance scaling factor. This allows understanding the evolution of the collision risk per event and predicting possible future probabilities after new orbital state updates.

In the analysed post-manoeuvre scenario, the target covariance size is dominated by the component in the in-track direction. Instead of varying the miss-distance vector and numerically maximising the collision probability, an analytical formulation for the worst-case in-track displacement is found. This is achieved by minimizing the miss distance vector $\Delta \boldsymbol{r}$ using a time offset Δt_t for the target state propagation.

The geometry around the time of closest approach is illustrated in Figure 4 and is described with the following equation:

$$\boldsymbol{r}_t + t_{t,\min}\boldsymbol{v}_t + \frac{\boldsymbol{v}_t \times \boldsymbol{v}_c}{|\boldsymbol{v}_t \times \boldsymbol{v}_c|} |\Delta \boldsymbol{r}|_{\min} = \boldsymbol{r}_c + t_{c,\min}\, \boldsymbol{v}_c ,$$

where $\boldsymbol{r}_c$ and $\boldsymbol{r}_t$ are the position vectors of chaser and target and $\boldsymbol{v}_c$ and $\boldsymbol{v}_t$ are the velocities at the original time of the closest approach. The time offset is parametrized using two different propagation times for each object, i.e. $\Delta t_t = t_{t,\min} - t_{c,\min}$.

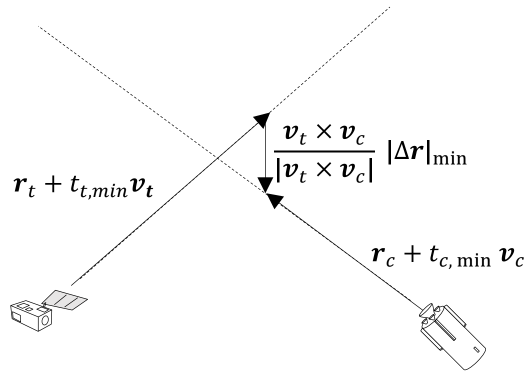

Figure 7: Illustration of close-approach geometry

The minimum miss-distance and time offset is then obtained by solving the linear equation system

$$\begin{pmatrix} \boldsymbol{v}_t & -\boldsymbol{v}_c & \frac{\boldsymbol{v}_t \times \boldsymbol{v}_c}{|\boldsymbol{v}_t \times \boldsymbol{v}_c|} \end{pmatrix} \begin{pmatrix} t_{t,\min} \\ t_{c,\min} \\ |\Delta \boldsymbol{r}|_{\min} \end{pmatrix} = \boldsymbol{r}_t - \boldsymbol{r}_c .$$

The time offset of this equation can take any arbitrary value. In order to model a worst-case scenario, the offset must be bounded using the large in-track uncertainty after the planned manoeuvre. A certain percentile of the normal distribution $N(0, \sigma_T)$, e.g. 99.9%, defines the maximum possible displacement along the in-track direction. If the offset Δt_t is larger than what can be reached within the uncertainty interval, the maximum value of the percentile is used instead. Afterward, the time of closest approach must be updated.

Finally, given the new approach geometry, the maximum probability is computed by varying in-track component of the covariance. For this purpose, the target covariance is decomposed into eigenvalue and eigenvectors, the eigenvalue corresponding to the eigenvector closest to the in-track direction is then set according to the bounds on the post-manoeuvre orbit determination uncertainty interval. Afterwards, the covariance is reassembled from the modified eigenvalues and eigenvectors and used for the collision probability. The numerical maximisation is then described with

$$P_{C,new} = \max_{\sigma_T} P_C(\sigma_T) ,$$

where the approach from [20] is used to compute the nominal collision probability.

3.2.3 Comparison of approaches

Historic conjunction data messages are used to assess the feasibility of the approaches and compare the number of high-risk events (effectively number of cancelled acquisition manoeuvres). In order to sample a reasonable distribution of chaser uncertainties and geometries, all CDMs between 3 and 1.5 days before the time of closest approach are extracted. As the database of events is dominated by ones without large manoeuvres, the uncertainties are artificially increased. The same eigenvalue decomposition approach as in the previous section is used to set the in-track standard deviation of the target covariance to ~5 km.

In a next step, the classical collision probability is recalculated for all messages together with the confidence interval and the new metric. The post-manoeuvre orbit determination in-track uncertainty is for the sake of simplicity varied within 50-100 m. In practise, a look-up table can be used to define reasonable bounds on the standard deviation. The in-track deviation is allowed to be in the central 99.9% interval (denoted p99.9 in the figures). Figure 8 compares the nominal collision probability P_C with new metric $P_{C,new}$. The metrics perfectly agree if a value is exactly on the diagonal. The new metric increases the collision probability for all points above the diagonal and consequently reduces it for the points below. Hence, in the majority of cases the probability is actually reduced to negligible level (values are cut at 1e-30) when using the new metric. The typical 1e-4 reaction threshold is illustrated using the blue solid line. In total ~5700 events are analysed, out of these two would have been identified as critical using the nominal approach. The new metric increases the number of required actions to 8.

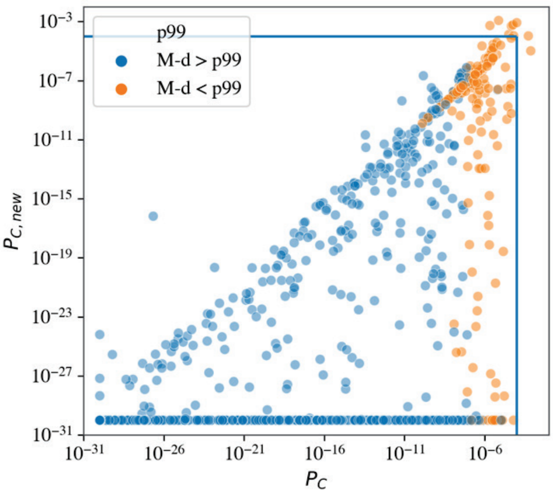

Figure 8: Comparison of nominal collision probability, new metric and confidence interval on miss distance vector. The solid blue line highlights the typical 1e-4 decision threshold. The displacement is constraint to be in the p99.9 interval.

Additionally, the colour coding of the figure illustrates whether the miss-distance is within the confidence interval (p99) or not. Using this approach around 204 conjunctions would have been classified as risky and could have led to a cancelled acquisition manoeuvre.

The impact of the decision threshold is analysed in Figure 9. The additional number of events which require an action w.r.t. the overall number of warnings stays approximately constant at 0.1% using the new metric. The confidence region approach requires 25-45 more additional actions.

To summarise: the new metric identifies an acceptable number of new events, which still allows manoeuvring to the target orbit. It achieves this while still giving the confidence that the new metric is a conservative value as it allows for large displacements and maximises the collision probability within feasible intervals.

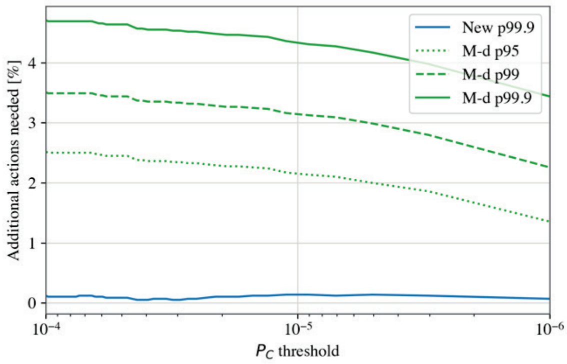

Figure 9: Threshold variation

4 CONJUNCTION EVENT STATISTICS

In this section we will provide some statistics on the identified conjunction events for the time period starting 2015, i.e. covering the time span after the data sharing agreement with the US was signed and CDMs for a large volume around the target trajectories have been obtained.

4.1 High risk events and avoidance manoeuvres

Figure 10 shows the number of conjunction events which triggered an alarm by the SDO analyst to the Flight Control Team of a mission covered by the support as well as the number of avoidance manoeuvres actually performed. It can be seen that for the fleet (see Figure 1) in the recent years there is on average about one to two manoeuvres per month and about three times as many alarms raised to the control team of a mission which triggers assessments and preparations of avoidance options. Figure 11 shows the classification of the conjunctions according to the highest collision risk observed throughout all CDMs received for an event. As expected, the number of events above the typical decision threshold of 10^{-4} is very low. For the majority of events (92%) the maximum estimated risk never exceeds 10^{-10}.

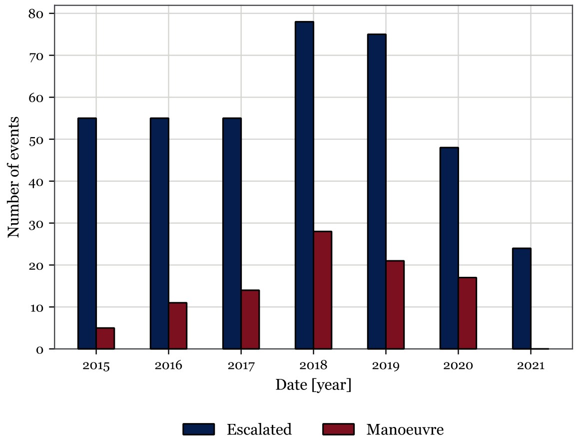

Figure 10: Number of conjunction events from 2015 – April 2021, escalated by the SDO analyst to the Flight Control Team of a mission and number of avoidance manoeuvres performed.

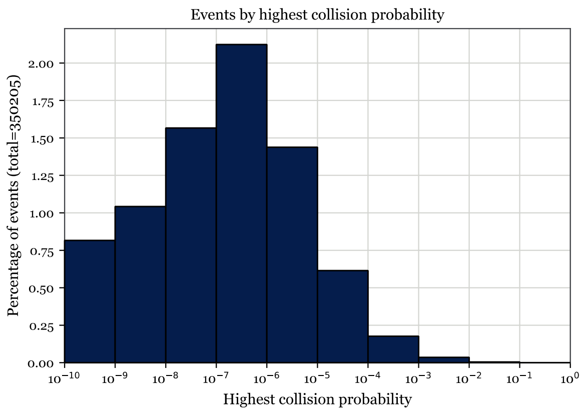

Figure 11: Distribution of the events as a function of the maximum collision probability (with max. probability at least 10^{-10}).

4.2 Class of the secondary objects

Figure 12 shows the distribution of categories of secondary objects for the registered events with at least one evaluation of the collision probability above 10^{-6}. Whereas in the earlier years the share of the large contributors Iridium-33 and Cosmos-2251 had been slowly decreasing (less so for FengYun 1C) and other payload fragmentation debris and payloads being on the rise, this has changed sharply in 2020 with the share of satellites jumping to ~50%, clearly dominated by constellation payloads.

This is driven by the accelerating deployment of the commercial payloads in LEO as is highlighted in Figure 13 and also driven by part of the ESA fleet orbiting below the operational altitude of the large constellations but above their injection altitude, i.e. those ESA spacecraft's altitudes are crossed by those constellation spacecraft during their initial orbit raise.

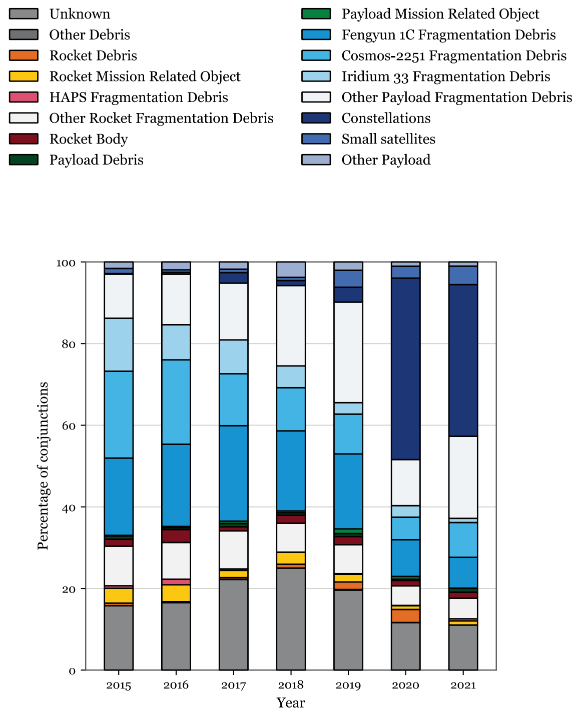

Figure 12: Distribution of secondary objects by class over time from 2015 – April 2021.

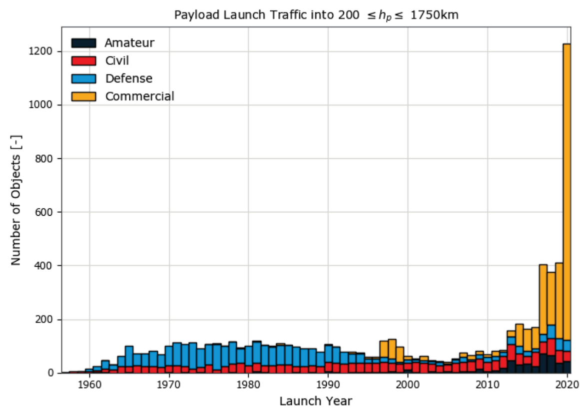

Figure 13: Evolution of the launch traffic to LEO per mission funding.

5 SUMMARY AND CONCLUSIONS

ESA's Space Debris Office (SDO) provides operational collision avoidance support to internal ESA missions as well as external partners. In this paper the current operational process has been described with a focus on how the building blocks connect to an overall largely automated process flow. As these connections have been implemented over time resulting in a complex system of scripts, the processing framework is currently being refactored. The modern software technologies used have been outlined, allowing to improve fault tolerance and repeatability, to increase performance and scalability and to provide a convenient UI for controlling the process.

The SDO also performs custom analyses to support non-standard scenarios and two of them were presented in this paper: an Earth flyby of interplanetary missions and manoeuvre campaigns involving large delta-vs where the usual approach of pre-manoeuvre screening quickly suffers from probability dilution due to large covariances induced by the manoeuvre uncertainties.

Finally, statistics of the conjunction data collected over the recent years have been presented, showing approximately one avoidance manoeuver every 2 to 4 weeks for the fleet covered and about 3times as many escalations to the control teams (i.e. approx. 1 out of 3 events the SDO escalates actually results in an avoidance manoeuvre). Moreover, the statistics shows also a step increase in the share of conjunctions with constellation spacecraft in 2020, clearly related to their accelerating deployment starting in 2020.

6 REFERENCES

1. Domínguez-González, R., Sánchez-Ortiz, N., Krag, H., Gelhaus, J. (2012). Analysis of uncertainties of catalogued orbital data for the update of the ESA DRAMA ARES tool. In *Proceedings of the 63rd International Astronautical Congress*.
2. Sánchez-Ortiz, N., Domínguez-González, R., Krag, H., Flohrer, T. (2015). Impact on mission design due to collision avoidance operations based on TLE or CSM information. *Acta Astronautica, 116, 368-381.*
3. Braun, V., Lemmen,s S., Bastida Virgili, B., Merz, K., Expected collision avoidance manoeuvre rates in DRAMA-ARES based on a history of Conjunction Data Messages, *69th International Astronautical Congress, 2018, IAC-18,A6,2,8,x44771*
4. Merz, K., Virgili, B. B., Braun, V. (2019). Risk reduction and collision risk thresholds for missions operated at ESA. *27th International Symposium on Space Flight Dynamics (ISSFD).*
5. Grande-Olalla, I., Sanchez-Ortiz, N., Pulido, J. A., & Merz, K. (2013, August). Collision Risk Assessment and Avoidance Manoeuvres for ESA. *6th European Conference on Space Debris, Darmstadt*, Germany.
6. Klinkrad, H., Alarcon, J. R., & Sanchez, N. (2005). Collision avoidance for operational ESA satellites. *4th European Conference on Space Debris*, Darmstadt, Germany.
7. Merz, K., Virgili, B. B., Braun, V., Flohrer, T., Funke, Q., Krag, H., Siminski, J. (2017). Current collision avoidance service by ESA's space debris office. *7th European Conference on Space Debris*, Darmstadt, Germany.
8. Braun, V., Flohrer, T., Krag, H., Merz, K., Lemmens, S., Virgili, B. B., Funke, Q. (2016). Operational support to collision avoidance activities by ESA's space debris office. *CEAS Space Journal, 8(3), 177-189.*
9. Celery Project (2021, April). Celery - Distributed Task Queue. https://docs.celeryproject.org/
10. Pallets Project (2021, April). Flask documentation. https://flask.palletsprojects.com/
11. Facebook Inc (2021, April). React - A JavaScript library for building user interfaces. https://reactjs.org/
12. Uriot, T., Izzo, D., Simões, L.F. et al. (2021). Spacecraft collision avoidance challenge: Design and results of a machine learning competition. *Astrodynamics, (2021).*
13. Mangano, V., Dósa, M., Fränz, M., Milillo, A., Oliveira, J. S., Lee, Y. J., et al. (2021). BepiColombo science investigations during cruise and flybys at the Earth, Venus and Mercury. *Space Science Reviews, 217(1), 1-81.*
14. Inter-Agency Space Debris Coordination Committee (2002). IADC Space Debris Mitigation Guidelines, IADC-02-01, Revision 1.
15. Alarcón Rodríguez, J. R., Martínez Fadrique, F., & Klinkrad, H. (2002, August). Collision Risk Assessment with a Smart Sieve Method. *In Joint ESA-NASA Space-Flight Safety Conference (Vol. 486, p. 159).*
16. Hejduk, M. D., Snow, D. E., Newman, L. K. (2019). Satellite conjunction assessment risk analysis for "dilution region" events: Issues and operational approaches, *Space Traffic Management Conference*, Austin, Texas, USA.
17. Balch, M. S., Martin, R., & Ferson, S. (2019). Satellite conjunction analysis and the false confidence theorem. *Proceedings of the Royal Society A, 475(2227).*
18. Kuchynka, P., Serrano, M. M., Merz, K., Siminski, J. (2020). Uncertainties in GPS-based operational orbit determination: a case study of the Sentinel-1 and Sentinel-2 satellites. *The Aeronautical Journal, 124(1276), 888-901.*
19. Alfano, S., Oltrogge, D. (2018). Probability of Collision: Valuation, variability, visualization, and validity. *Acta Astronautica, 148, 301-316.*
20. Akella, M. R., & Alfriend, K. T. (2000). Probability of collision between space objects. *Journal of Guidance, Control, and Dynamics, 23(5), 769-772.*